*35th EPS Conference on Plasma Phys. Hersonissos, 9 - 13 June 2008 ECA Vol.**32D**, P-5.158 (2008)*

Coexistence of the drift wave spectrum and low-frequency zonal flow potential in cylindrical laboratory plasmas

Y. Nagashima[1], S.-I Itoh[2], S. Shinohara[2], M. Fukao[3], A. Fujisawa[4], K. Terasaka[2], T. Nishijima[2], M. Kawaguchi[2], Y. Kawai[2], N. Kasuya[4], G.R. Tynan[5], P.H. Diamond[5], M. Yagi[2], S. Inagaki[2], T. Yamada[1], K. Kamataki[2], M. Maruta[2], and K. Itoh[1]

[1] *Univ. Tokyo, Kashiwa, Japan,* [2] *Kyushu Univ., Kasuga, Japan,* [3] *Myojo-cho, Uji, Japan,* [4] *NIFS, Toki, Japan,* [5] *UCSD, La Jolla, USA*

Introduction

Physics of zonal flows and their interaction with turbulence is one of the most attractive research fields in fusion plasma confinement and its control [1]. The zonal flow is considered to be exclusively driven by nonlinearity of micro-scale turbulence, and to affect turbulence transport. However, many experimental research tasks for understanding the zonal flow physics are left; How does the zonal flow distribute radially, where is the zonal flow excited and damped, and how is turbulence affected by the zonal flow? In the Large Mirror Device of Kyushu University [2], a low-frequency zonal $\mathbf{E}\times\mathbf{B}$ velocity ($\mathrm{ZV}_{\mathbf{E}\times\mathbf{B}}$) is observed as well as the drift wave spectrum (DW), and details of coexistence of the $\mathrm{ZV}_{\mathbf{E}\times\mathbf{B}}$ and the DW has been investigated. The Large Mirror Device (LMD) is a basic plasma experiment device shown in Fig. 1(a), which has a cylindrical vacuum vessel made of stainless steel with a linear magnetic field configuration up to 0.12 [T]. Helicon plasmas are produced by an RF source (2 kW) at one end of the vacuum vessel. Fluctuations are mainly measured with a Reynolds stress probe (RSP) shown in Fig. 1(b), located at 60 cm far from the source region where axial density profile is stable. Three electrodes in the RSP are used for the floating potential fluctuation $\tilde{\Phi}_\mathrm{f}$ measurement and Reynolds stress term $\langle\tilde{v}_r\tilde{v}_\theta\rangle$ assuming that $\mathbf{E}\times\mathbf{B}$ velocity is dominant as the plasma velocity. In this paper, we show detail features of the $\mathrm{ZV}_{\mathbf{E}\times\mathbf{B}}$ and the DW , and nonlinear interactions between them in the LMD.

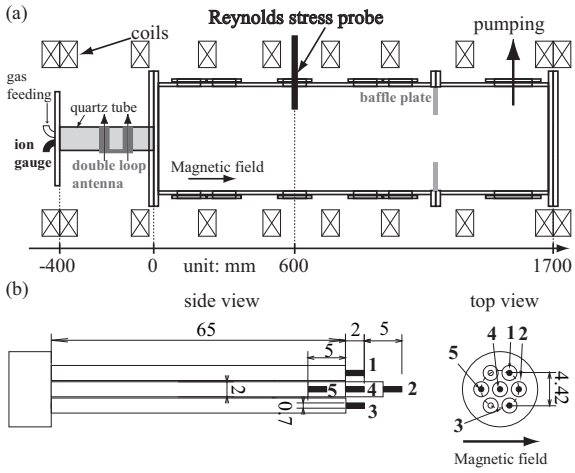

Figure 1: (a) The Large Mirror Device, and (b) the Reynolds stress probe.

Quadratic spectra of the zonal $\mathbf{E}\times\mathbf{B}$ velocity and the drift wave

The coexistence of the $ZV_{\mathbf{E}\times\mathbf{B}}$ and the DW is observed in the vicinity of a phase transition in which the fluctuation behaviors change from combination of coherent spectral peaks to the broadband spectrum. The phase transition occurs spontaneously as the magnetic field strength B increases with the filling Ar gas pressure P_{Ar} fixed and/or as P_{Ar} reduces with B fixed. In this operation, B=0.12 [T] and P_{Ar} ∼3.5 [mTorr]. Figure 2 shows a comparison of spectrum between the normalized ion saturation current fluctuation $\tilde{I}_{\mathrm{i,sat}}/\overline{I_{\mathrm{i,sat}}}$ and the normalized floating potential fluctuation $\tilde{\Phi}_{\mathrm{f}}/\overline{T_{\mathrm{e}}}$, where $\overline{T_{\mathrm{e}}}$ is the equilibrium electron temperature. Two distinctive spectral peaks are observed at ∼0.4 and 7-8 kHz. We abbreviate the former and the latter fluctuations as the $ZV_{\mathbf{E}\times\mathbf{B}}$ and the DW, respectively. Confirmations are described in following sentences.

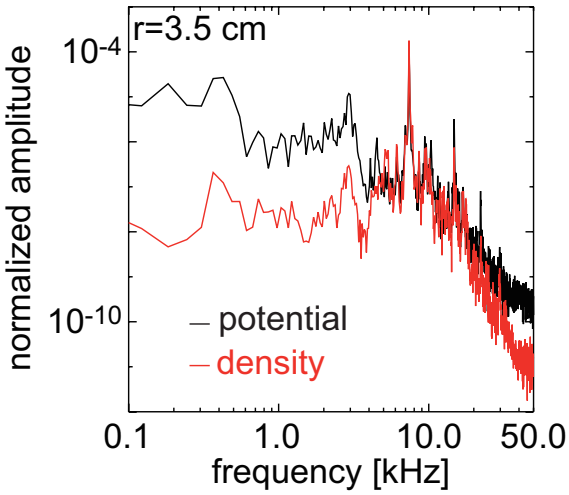

Figure 2: Autopower spectra of normalized fluctuation amplitude. The floating potential fluctuation amplitude (black) and the ion saturation current amplitude (red).

The $ZV_{\mathbf{E}\times\mathbf{B}}$ has larger potential amplitude than density. The two-point cross-phase analysis shows that the poloidal and the axial cross-phases of the $ZV_{\mathbf{E}\times\mathbf{B}}$ is within $\pm 0.2\,[\mathrm{rad}/2\pi]$, consistent with the poloidal/axial mode numbers $m/n = 0/0$. The DW has features different from the $ZV_{\mathbf{E}\times\mathbf{B}}$. The DW normalized amplitude of potential is similar with that of density, and wave numbers of the DW are finite (m/n=3-5/2-3). These features does not contradict that the DW is the drift wave. Figure 3(a) shows radial profile of the radial wave number k_r of the $ZV_{\mathbf{E}\times\mathbf{B}}$. The $ZV_{\mathbf{E}\times\mathbf{B}}$ has finite radial wave numbers at the radial location r=∼2 and 4 cm. However, we also observe inversion of polarity in the $ZV_{\mathbf{E}\times\mathbf{B}}$ k_r relative to the location of maximal DW amplitude. On the other hand, Figure 3(b) shows radial profile of k_r of the DW. Signs of the

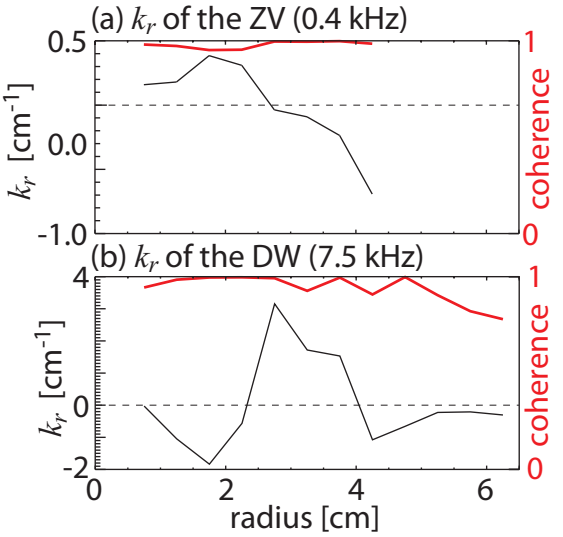

Figure 3: Radial profiles of radial wave numbers. (a) the $ZV_{\mathbf{E}\times\mathbf{B}}$, and (b) the DW. Radial wave numbers are derived by the two-point cross-phase analysis.

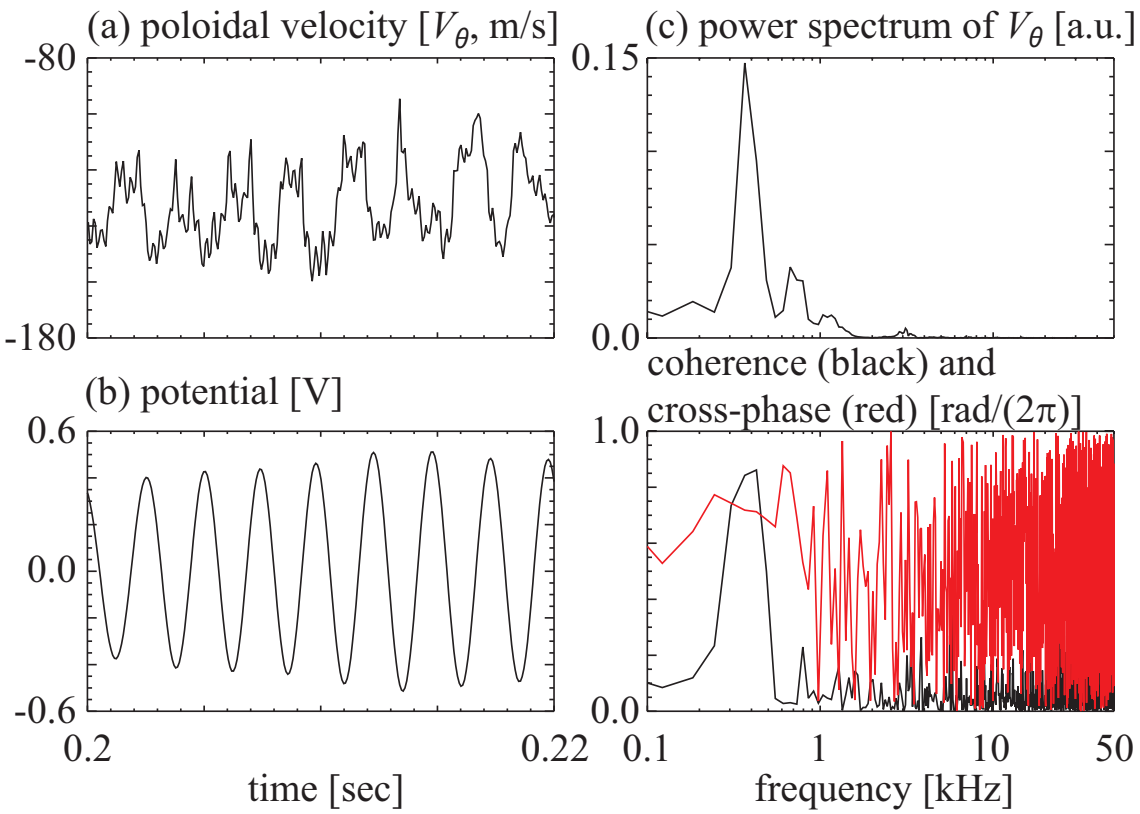

Figure 4: Information of poloidal velocity fluctuation associated with the $ZV_{\mathbf{E}\times\mathbf{B}}$ oscillation. (a) $\tilde{V}_\theta(t)$ measured by the TDE analysis, (b) $\tilde{\Phi}(t)$ for $ZV_{\mathbf{E}\times\mathbf{B}}$, (c) power spectrum of $\tilde{V}_\theta(t)$ and (d) the cross-coherence and the cross-phase between $\tilde{V}_\theta(t)$ and $\tilde{\Phi}(t)$. A time window $\tau_{\rm TDE}$ for the TDE analysis is 512 [μsec] ($\tau_{\rm ZV} > \tau_{\rm TDE} > \tau_{\rm DW}$), and results from quadratic spectra is valid for $f <\sim 2$ kHz.

k_r polarity change radially, indicating that k_r of the DW is modulated spatially (a vortex tilting). Linear dispersion relation of the DW is calculated. Using observed parameters at the radial location where the DW amplitude has a maximum, we evaluate the drift wave frequency $\omega_{\rm DW}$=$\omega^*/(1+k_\perp^2\rho_{\rm s}^2)$=6-8 kHz, where $\omega^* = k_\theta T_{\rm e}/(eB\lambda_n)$, $k_\perp$ is the wave number perpendicular to the magnetic field, $\rho_{\rm s}$ is the ion Larmor radius at the electron temperature, k_θ is the poroildal wave number, and λ_n is the density scale length. The calculation of frequency is consistent with the spectral peak frequency of the DW 7-8 kHz.

Details of the zonal E $\times$ B velocity

Potential analysis is not enough for identifying the zonal flow. Definition of the zonal flow is an poloidal ion flow velocity, therefore, other poloidal flow measurements can test whether the $ZV_{\mathbf{E}\times\mathbf{B}}$ is the zonal flow or not. Supported by the Time Delay Estimation analysis [3], the poloidal flow oscillation of turbulent fluctuations associated with the $ZV_{\mathbf{E}\times\mathbf{B}}$ is evaluated. Figure 4 shows results of the poloidal velocity fluctuation $\tilde{V}_\theta(t)$ derived from the TDE analysis and their relationship with the potential fluctuation for the $ZV_{\mathbf{E}\times\mathbf{B}}$. Two plots of $\tilde{V}_\theta(t)$ and $\tilde{\Phi}_{\rm f}(t)$

demonstrate a synchronization of $\tilde{V}_\theta(t)$ and $\tilde{\Phi}_\mathrm{f}(t)$ at the $\mathrm{ZV}_{\mathbf{E}\times\mathbf{B}}$ frequency, shown in Fig. 4. Testing significance of the synchronization by cross-correlation analysis, we observe a significant spectral peak of the squared coherence between $\tilde{V}_\theta(t)$ and $\tilde{\Phi}_\mathrm{f}(t)$ at the $\mathrm{ZV}_{\mathbf{E}\times\mathbf{B}}$ frequency. We confirm that the synchronization is statistically admissible. The cross-phase between potential and $\tilde{V}_\theta(t)$ is different in radius.

Nonlinear interaction between the $\mathrm{ZV}_{\mathbf{E}\times\mathbf{B}}$ and the DW

The bispectral analysis [4] can also demonstrate significance of nonlinear three-wave interaction, and is applied to nonlinear interaction between the zonal flow and turbulence. Figure 5 shows auto-bicoherence plot of the floating potential fluctuations, normalized $\langle\tilde{\Phi}_\mathrm{f}(f_1)\tilde{\Phi}_\mathrm{f}(f_3-f_1)\tilde{\Phi}^*_\mathrm{f}(f_3)\rangle$, at frequency 3 = 0.366 kHz (frequency of the $\mathrm{ZV}_{\mathbf{E}\times\mathbf{B}}$). A significant spectral peak at $f_1 \sim$7-8 kHz confirms that the $\mathrm{ZV}_{\mathbf{E}\times\mathbf{B}}$ is nonlinearly coupled to the DW.

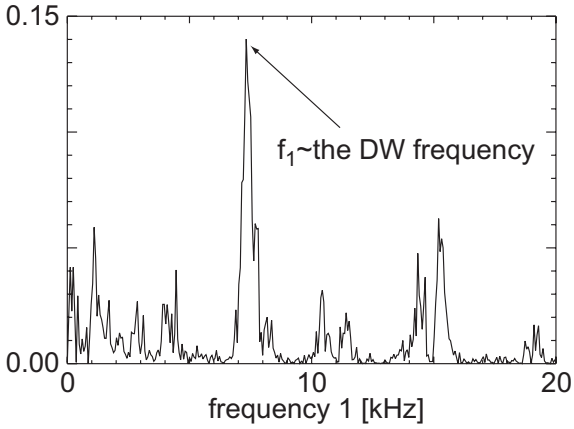

Figure 5: Auto-bicoherence of floating potential fluctuation at frequency 3 = 0.366 kHz (frequency of the $\mathrm{ZV}_{\mathbf{E}\times\mathbf{B}}$). Horizontal axis indicates frequency 1. Significance level is $\sim$0.002

Acknowledgment

This work was partially supported by Grant-in-Aid for Specially-Promoted Research (16002005) [Itoh project], and Grant-in-Aid for Scientific Research (18760637) of MEXT Japan. Support of all members of Itoh Laboratory, Yagi Laboratory, Kawai Laboratory and Tanaka Laboratory in carrying out the experiments is appreciated.

References

[1] P.H. Diamond, et al., Plasma Phys. Control. Fusion **47**, R35 (2005)

[2] Y. Saitou, et al., Phys. Plasmas **14**, 072301 (2007)

[3] C. Holland, et al., Phys. Rev. Lett. **96**, 195002 (2006)

[4] Y. Kim and E. Powers, IEEE Trans. Plasma Sci. **PS-7**, 120 (1979)